CONTRIBUTIONS to SCIENCE, **1** (2): 175-192 (1999)
Institut d'Estudis Catalans, Barcelona

Crustal accretion at mid-ocean ridges and backarc spreading centers: Insights from the Mid-Atlantic Ridge, the Bransfield Basin and the North Fiji Basin

Eulàlia Gràcia* and Javier Escartín**
Institut de Ciències de la Terra – Jaume Almera. Consell Superior d'Investigacions Científiques (CSIC), Barcelona

Abstract

Mid-Ocean Ridges are a natural laboratory for the study of magmatic and tectonic processes and their interactions. Owing to their relatively simple structure and geodynamic history, they have been studied by highly active projects, such as RIDGE (USA), followed by the international initiative InterRidge, which have yielded enormous advances during the last two decades. By these ridge-oriented initiatives, a large portion of the global ridge system has been explored, mapped and sampled. These data have constrained models of melt production and dynamics of the mantle, formation of the lithosphere, magmatic accretion of the crust, tectonic deformation, and volcanic processes at shallow levels, as well as their interactions. Geophysical observations (bathymetry, acoustic backscatter, and gravity) from several sites along mid-ocean ridges (Mid-Atlantic Ridge) and two back-arc basins (Bransfield and North Fiji) summarized here provide constraints on the surface expression of ridge tectonism, volcanism, and the density structure of the oceanic lithosphere in depth, and their bearing on the accretionary processes at ridges.

Resum

Les dorsals mèdio-oceàniques són laboratoris naturals per a l'estudi dels processos volcànics i tectònics, i les seves interaccions. La estructura i història geodinàmica relativament senzilla de les dorsals oceàniques ha fet que aquéstes siguin el focus d'actius projectes pluridisciplinars, tals com RIDGE (EUA), i InterRidge. Fonamentats en aquestes iniciatives en els darrers vint anys s'han produit avanços significatius, en l'exploració, cartografia i mostreig d'una elevada porció del sistema global de dorsals oceàniques. Aquestes dades han servit per a constrényer models de dinàmica del mantell i el seu percentage de fusió, de formació de la litosfera, d'acreció magmàtica, de deformació tectònica i dels processos volcànics en nivells superficials. Aquest és un article de síntesi en el qual agrupem observacions i interpretacions basades en la nostra pròpia experiència en diverses localitats al llarg de dorsals medio-oceàniques (Dorsal Mèdio-Atlàntica) i conques de rerearc (Bransfield i Nord-Fiji). Les eines utilitzades estan basades en els mètodes de geofísica marina comunment utilitzats en l'estudi de dorsals, com són la batimetría multifeix, la retrodifusió acústica, i la gravimetría. Els resultats d'aquests estudis ens proporcionen informació sobre la expressió superficial de la tectònica, volcanisme, així com de l'estructura en profunditat de la litosfera oceànica i els processos que hi tenen lloc.

Key words: Oceanic crust, spreading ridge, backarc, segmentation, faulting, volcanism

The oceanic crust, that covers more than 60% of the total Earth's surface, is the result of magmatic accretion which takes place along the global Mid-Ocean Ridge (MOR) system (Fig. 1) [1]. MORs, with a total length >70.000 km, are the locus of the most active and voluminous magmatic activity on the Earth, with a total production of more than 20 km^3 of oceanic crust every year, and contributes to two thirds of the total internal heat lost by the Earth. This magmatism directly results from the passive upwelling of the mantle and decompression melting as plates separate along the ridge axis. The ridge system is also one of the most tectonically active areas on Earth. Plate separation is taken up primarily by magmatic accretion (formation of oceanic crust), but also by tectonic extension of the lithosphere near the MOR, which produces an ubiquitous shallow seismicity belt along ridges, modifies the structure of the crust and morphology of the

* Author for correspondence: Eulàlia Gràcia, Institut de Ciències de la Terra – Jaume Almera (CSIC), Departament de Geofísica. Lluís Solé i Sabarís s/n. 08028 Barcelona, Catalonia (Spain). Tel. 34 93 409 54 10, Fax: 34 93 411 00 12. Email: egracia@ija.csic.es
** Now at: Laboratoire de Pétrologie, CNRS. Paris

seafloor. The morphology of the oceanic seafloor and structure and composition of the crust are thus a result of the interplay between magmatism, tectonism and hydrothermalism, and their study can provide constraints on the different processes occurring at MORs.

Here, we present data from two geodynamic settings with continuous generation of oceanic crust: mid-ocean ridges and backarc basins (Fig. 1). Regarding the first setting, we have selected three portions of the Mid-Atlantic Ridge (MAR), which show strong differences in shallow and deep structure according to the magmatic supply and the distance from hotspots. Regarding the second, two contrasting backarc basins have been selected, the Bransfield Basin (BB), with continental rifting and incipient accretion of oceanic crust, and the mature North Fiji Basin (NFB), where seafloor spreading processes are similar to those observed at MORs (Fig. 1).

Overview of Oceanic Crust Accretion

The relevance of the oceanic crust to understand plate tectonics and mantle convective processes, which was shown in the 1960's, raised intense research on mid-ocean ridges. The first surveys showed that MORs are a linear chain elevated 2-3 km above surrounding, older ocean basins as a result of thermal uplift due to mantle convection. New, more sophisticated surveying techniques, have revealed that the ridge is not continuous but dissected by a series of fracture zones [1,2]. With new swath-bathymetric systems, other ridge discontinuities at smaller scales [3] have been identified (e.g., overlapping spreading centers (OSCs) [4], nontransform offsets (NTOs) [5], and propagators [6]).

These studies have also shown that fast– and slow-spreading ridges display notable differences in segmentation, seafloor morphology, crustal structure, lithospheric composition, and nature of magmatic and tectonic processes. Spreading rate seems to be an important parameter controlling mantle upwelling, melt production and lithospheric cooling under ridge axis:

Ridge segmentation. One of the first observations revealed the presence of ridge segments, typically 40 km long (between 10 and 100 km) at the slow-spreading MAR, with transform discontinuities and NTOs displacing the axis laterally by <10 km and several hundred kilometers [e.g., 3]. In contrast, fast-spreading ridges show long, straight ridge sections (>100 km) with small lateral offsets (OSCs and propagators) or large offset fracture zones, and rotating microplates [e.g., 7].

Seafloor morphology. Slow-spreading ridges are characterized by a prominent rift valley (Fig. 2a), >1 km high typically, bounded by inward-facing normal faults [8]. The result of spreading and tectonic extension is the formation of abyssal hills sub-parallel to the ridge axis, with vertical reliefs ranging from several hundreds of meters and >2 km. In contrast, fast-spreading ridges are characterized by an axial high with a central summit caldera <50 m in vertical relief (Fig. 2a). Faulting seems to be less prominent, with abyssal hills of lesser amplitude.

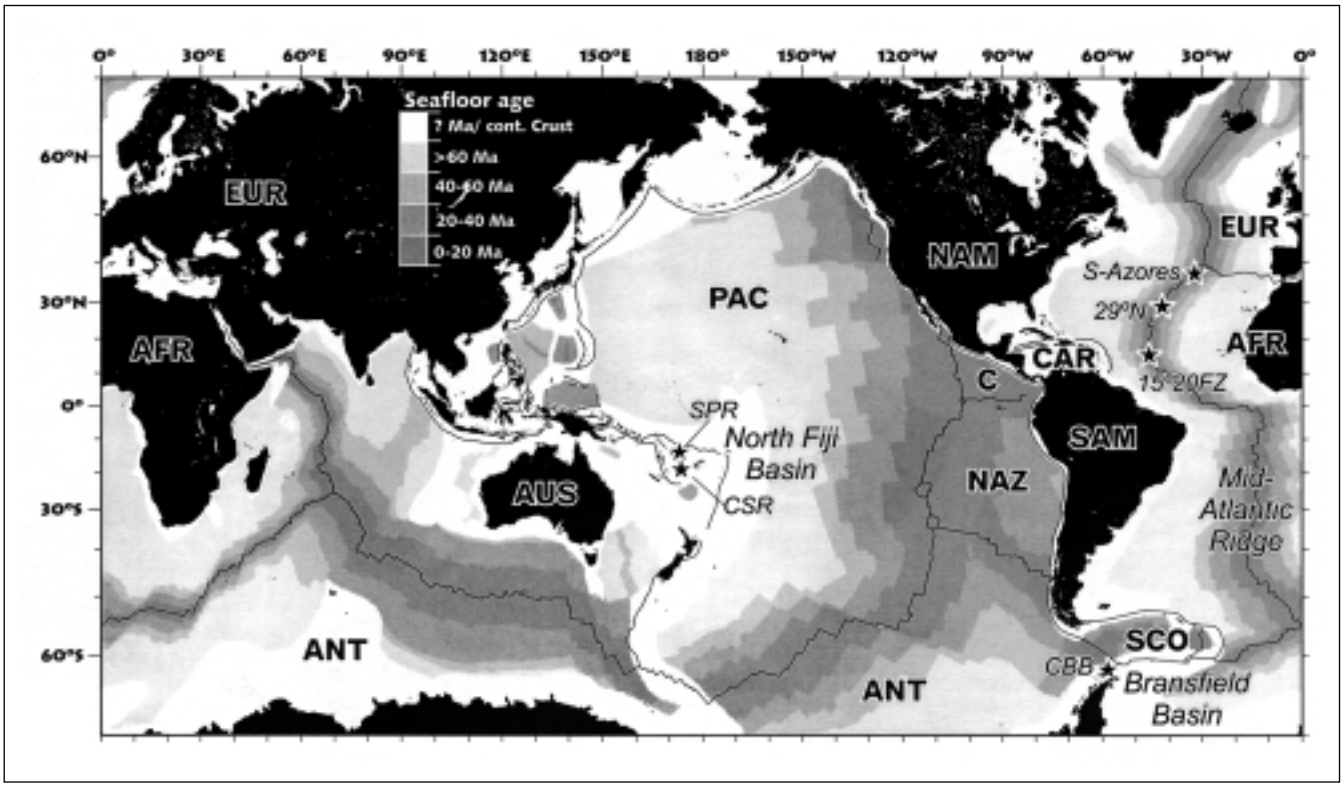

Figure 1. Seafloor age map [1] showing the location of the areas described in the text. Stars correspond to the study areas: CSR, Central Spreading Ridge; SPR, South Pandora Ridge; CBB, Central Bransfield Basin. Names of tectonic plates: PAC, Pacific; NAZ, Nazca; C, Cocos; SAM, South America; NAM, North America; EUR, Eurasia; AFR, Africa, AUS, Australia; ANT, Antarctica.

Crustal structure and composition. Slow-spreading ridges show high lateral variability in crustal composition and thickness. The crust is systematically thicker at the center of segments and thins towards the ends [e.g., 9-11] (Fig. 2b). Peridotites and gabbros are commonly dredged near the end of segments, suggesting that deep lithospheric levels are exposed on the seafloor by tectonic extension [12-14] and/or that the crust is not fully magmatic but highly heterogeneous and composed of gabbros and peridotites [15,16]. In contrast, the crustal thickness at fast-spreading ridges does not seem to vary substantially for hundreds of kilometers [e.g., 17,18] (Fig. 2b), and the scarcity of peridotite outcrops together with gravity and seismic data suggests that the crust is fully igneous and relatively homogeneous, with layers of gabbro, diabase and basalt (from bottom to top) overlying the mantle [19].

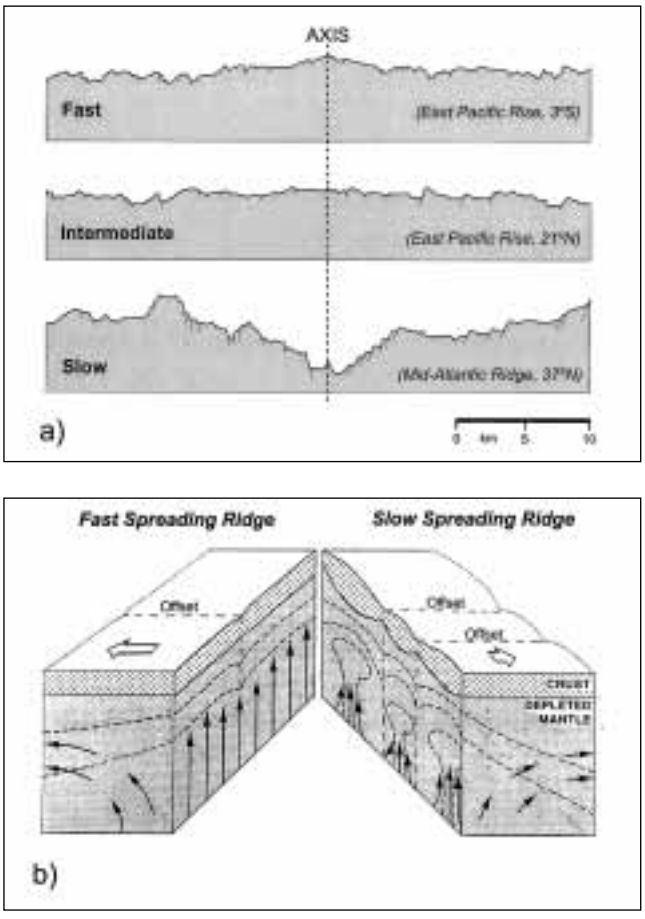

Figure 2. The morphology of the ridge crest (a) and the mode of mantle and/or melt flow and crustal accretion below the mid-ocean ridge (b) depend largely on spreading rate. a) Fast-spreading ridges (full-spreading rate > 60 mm/yr) typically show an axial high (< 500 m) with a small summit caldera (< 1 km wide). In contrast, slow-spreading ridges (full-spreading rate < 30 mm/yr) show a marked rift valley (typically 1 km deep or more), while intermediate ridges have transitional morphology. Modified from [5]. b) Slow-spreading ridges are characterized by transform discontinuities and NTOs that are segmented along the ridge axis at scales of 40-100 km. Segments show systematic variations in crustal thickness along their length as a result of focused magmatic accretion in depth (mantle convection and/or melt focusing). Fast-spreading ridges, in contrast, are characterized by a relatively constant crustal thickness and an inferred two-dimensional passive mantle upwelling and melt supply to the ridge axis. Modified from [24].

Magmatic and tectonic processes. The differences described above are caused by the effect of spreading rate on a) the thermal structure of the lithosphere and therefore on the mechanical properties and extensional tectonics at the ridge, and b) on the style of mantle upwelling and therefore, melt supply to the ridge axis. High melt supply to the ridge axis at fast-spreading ridges is indicated by the presence of a steady-state magma chamber [20,21] and by the evidence of abundant off-axis volcanism [e.g., 22], and volcanic eruptions [e.g., 23]. There is also a marked change in the style of magmatic accretion, from a laminar mode at fast-spreading ridges to a segmented, plume-like mode at slow-spreading ridges [24] (Fig. 2b). This may arise from buoyant segmentation of mantle upwelling at slow-spreading ridges [e.g., 9,24,25,26]. Alternatively, segmentation may occur at shallow levels in the melt extraction process [25,27]. Differences in the thermal regime also explain the transition observed from an axial high at fast spreading ridges to an axial valley at slow spreading ridges [28,29,30] (Fig. 2a).

Data and Methods

Geophysical methods and geological observations are essential tools to study mid-ocean ridges and backarc spreading centers. We can consider three main working scales for the most usual methods:

1) Global. Satellite altimetry data provide the gravity field over the oceans, including large areas of uncharted seafloor, such as southern oceans and Antarctic margins [31].
2) Regional. Shipboard data (swath-bathymetry/acoustic backscatter, magnetics, gravity, seismics, electromagnetic) provide high-resolution (100-10 m) coverage over regions at 100-km scales. These data allow the identification of detailed volcanic and tectonic features of the seafloor, as well as deep structure (i.e., velocity, density) of the oceanic lithosphere.
3) Local. Remotely operated vehicles (ROVs), and autonomous underwater vehicles (AUVs), such as manned submersibles provide *in situ* data (<1-10 m resolution) for studying magmatic and tectonic features at local scales (1-10 km). A summary of the main methods and systems used in mid-ocean ridge surveys is presented on Table 1.

In this paper, we focus on the seafloor structures and on the shallow density structure of the oceanic lithosphere at ridges, characterized from swath-bathymetry acoustic backscatter data and from gravity data, respectively. Satellite gravity data provide a regional perspective of the tectonic structures and setting for each of the study areas: the slow-spreading MAR (South of the Azores, South of Atlantis FZ, and Fifteen-Twenty, Table 2), and three backarc areas (South Pandora Ridge and Central Spreading Ridge in the North Fiji Basin, and Central Bransfield Basin, Table 2).

Table 1. Methods commonly used in mid-ocean ridge surveys, especially the ones followed here.

Method	*Measurement accuracy*	*Data output*	*Main results on M.O.R.*	*Systems commonly used in M.O.R. surveys*
satellite altimetry	>1 km	sea-surface height	global scale gravity and bathymetry	GEOSAT/GM, ERS-1/GM, SEASAT, TOPEX
shipborne				
swath-bathymetry	100 -150 m	water-depth, acoustic backscatter	morphostructure, seafloor facies	Simrad EM1000 and EM12 (Norway) Seabeam 2000 (USA), Thomsom (Fr) Furuno HS10 (Jap.), Hydrosweep (USA)
side-scan sonar	50-100 m	acoustic backscatter	seafloor facies, tectonic/magmatic mapping	GLORIA (UK) HMR-1 (USA)
gravity	1 km	gravity field / anomalies (FAA, MBA)	relative crustal thickness	Bodenseewerk KSS330
magnetics		magnetic field / anomalies	spreading rate, crustal magnetization	EGG-Geom. G866, BGM3 Barringer M244 proton magnetometre
near-bottom				
deep tow	<1-10 m	bathymetry, backscatter, magnetics, video, photo	high-res. morphostructure, detailed geophysical surveying	TOBI (UK), SAR (Fr), DSL-120 (USA)
ROVs*	0.1-5 m	bathymetry, backscatter, magnetics, video, photo, rock and water sampling	seafloor monitoring, sampling, in situ geophysics	Jason (USA), Ropos (Can.), Victor (Fr.)
AUVs** / submersibles	0.1-5 m	bathymetry, backscatter, magnetics, video, photo, rock and water sampling	direct observation, geological mapping / sampling hydrothermal activ. exploration	Alvin, ABE (USA), Cyana, Nautile (Fr), Shinkai 2000, Shinkai 6500 (Japan), MIR-I, MIR-II (Rus.)

*ROV: Remotely Operated Vehicle
**AUV: Autonomous Underwater Vehicle, such as manned submersibles, which allow scientists to go up to 6.500 m deep.

The Slow-Spreading Mid-Atlantic Ridge

The MAR has been extensively studied during the last 25 years, from the Equatorial MAR to the Iceland hotspot. We have chosen three sites along the MAR: a hotspot-influenced magmatic ridge section (South Azores), a «normal» ridge section away from hotspots (South Atlantis FZ) and a «cold» section (Fifteen-Twenty) were spreading is mostly amagmatic (Figs. 1, 3a). The spreading rate in the three areas is very similar (24-26 mm/yr full rate, Table 2), and variations in morphology, tectonic structure and crustal composition maybe directly linked to magma supply.

MAR South of the Azores, 38°N-35°40'N

The MAR south of the Azores is especially interesting for the study of ridge-hotspot interactions (Figs. 1, 3a). First, it is close to the Azores hotspot and so affected by the associated thermal and chemical flux [32]. Second, at a smaller scale, the ridge comprises several varying ridge segments linked by systematic left-lateral NTOs [33,34]. The regional pattern of MAR between 38°N and 35°40'N has been outlined by [34]. Along this ±500 km long section of the ridge, with a general trend of 050°, and average full spreading rate of 22 mm/yr, there is a relatively constant along-axis topographic gradient from the Azores platform towards the south [34,35] (Fig. 3b).

In a regional sense, the MAR south of the Azores is segmented by two large discontinuities, the Pico and Oceanographer Fracture Zones, which include seven second-order segments separated by large and wide NTOs. The northernmost segments are strongly influenced by the Azores hotspot, and the rift valley, which typifies most slow-spreading ridges, disappears. All the ridge segments are associated with Mantle Bouguer anomaly (MBA) gravity lows, but show less along-axis variation than in other sections of the MAR [34,35].

In order to determine the interaction and balance between extrusive volcanic activity and extensional tectonics, the segments and NTOs of the MAR south of Azores (38°N to 35°40'N) were imaged using the Towed Ocean Bottom Instrument (TOBI) [36] (Table 1). Volcanic-tectonic terrains present various degrees of tectonic dismemberment and deformation, a range of sedimentary cover and thickness, and relationships between lava flows, providing us with a relative age between them. In many cases, groundtruthing of these terrains was carried out with a combination of submersible observations, deep-tow camera traverses and dredge sampling [37-39]. The three main geological categories (volcanic, tectonic and sedimentary) of the TOBI seafloor textures [40] are shown in Figure 4a.

The segment presented in this work, named Lucky Strike, is characterized by rift valley morphology, showing a fairly constant width of 11-12 km throughout its 60 km of length (Fig. 3b). The dominant bathymetric feature is the shallow platform area, which occupies 50 km^2 of the central axial floor between 2100 and 1800 m water depth. Its gently sloping upper surface is topped with four small volcanoes/volcanic ridges [39]. On the TOBI sidescan sonar image of this

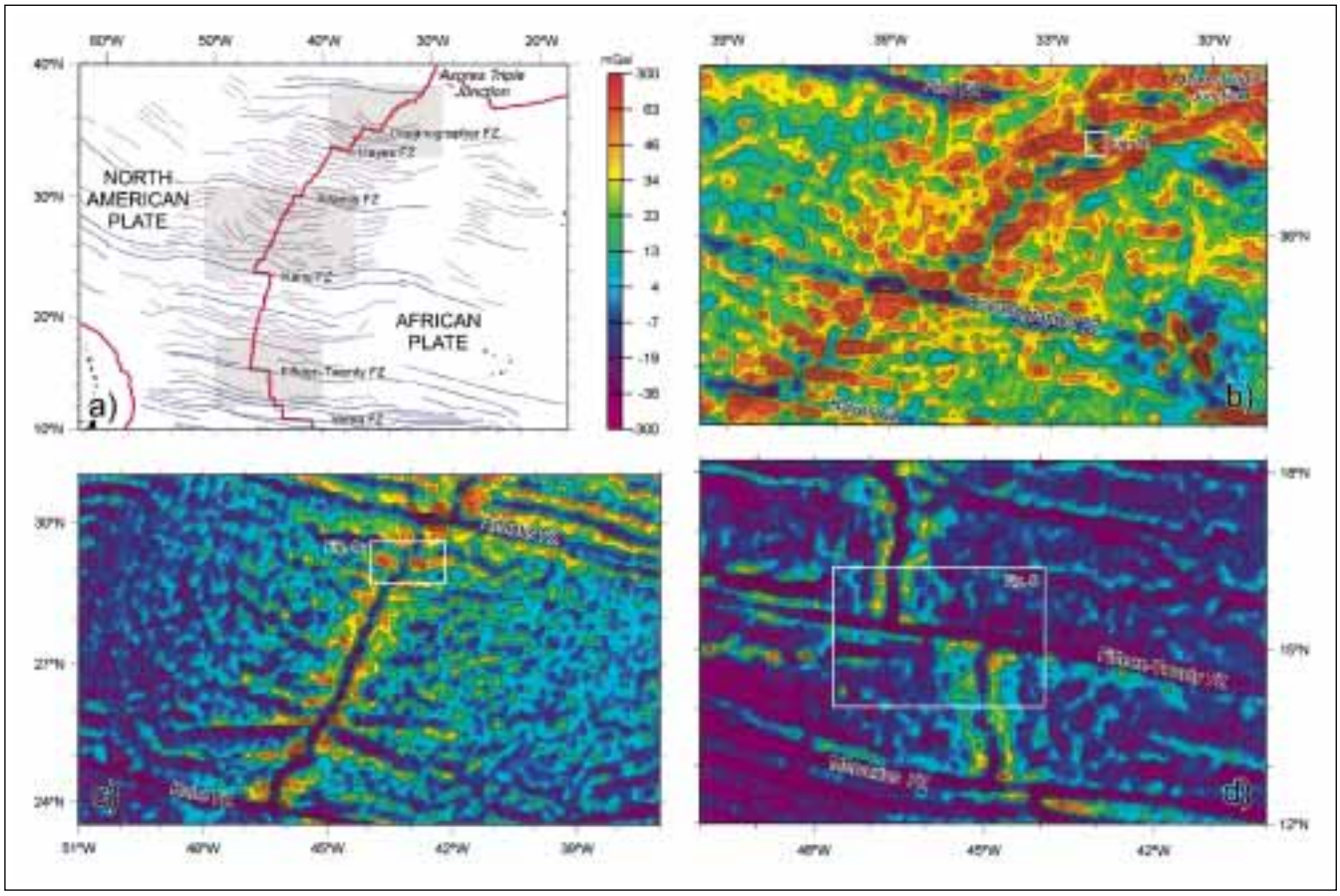

Figure 3. a) Location map of the three selected areas along the Mid-Atlantic Ridge: b) South of Azores, extending from the Azores to the Oceanographer FZ, c) 29°N, extending from Atlantis FZ to Kane FZ and d) around the 15°20'N FZ. Data in b-d) are based on satellite gravity map [31]. Location of Figs. 4b, 4c and 5 are also depicted.

segment (Fig. 4b), the central volcano cluster, characterized by volcanic breccia and pillow constructs, is cut by several fault/fissure lineaments which continue across the platform [37,38]. The platform surface, characterized by a mottled/patchy backscatter pattern, is cut through almost everywhere by a fabric of closely spaced faults and fissures, with less than 25 m vertical throw [40]. To the north and south of the platform, TOBI data show well-defined linear clusters of constructional volcanic ridges consisting of numerous pillow mounds [38]. This mounded terrain is locally cut by dense arrays of faults, but the style of faulting varies systematically when the distance from the segment center increases (Fig. 4b). Away from the centre, the number of faults decreases, show a larger spacement (more than 250 m), and have greater individual throws (between 50 and 75 m) [40]. Faulting in the northern domain follows a similar pattern, but is not as widespread. Both domains contain small lava flows, either pervasively faulted or completely undeformed. In both areas, overlapping flow margins provide unequivocal evidence for complex, multiple extrusive events.

MAR South of Atlantis Fracture Zone, 29°N

The Broken Spur segment is ~80 km long, limited by the 29°23'N and 28°51'N NTOs (Fig. 3a,c), and shows the characteristics of a «typical» slow-spreading segment. Traces of the NTOs bounding the segment to the north and south [41], demonstrate that the offsets have migrated along the axis. Several geophysical studies have described its morphology [33,42-44], gravity and crustal structure [9,41], and tectonic evolution [45]. The crust at the segment center is thicker than at the end [9]. In addition, there is an across-axis asymmetry at the segment end, with thicker crust at the outside corner (OC) than at the inside corner (IC) of ridge-offset intersections [9,41], reflecting the combined effect of focused magmatic accretion on axis [e.g., 9,46] and tectonic thinning at ICs [47]. The IC terrain is characterized by larger faults (>1 km in throw) than the OC or segment center (SC) (<500 m) [43,48], and is associated with diffuse microseismic activity [49].

Variations in tectonic strain and faulting along and across the segment are characterized from high-resolution TOBI sidescan sonar data (Fig. 4c). TOBI backscatter data allow the identification of individual faults, the measurement of fault width and spacing, horizontal fault displacement (heave), and tectonic strain [50]. Over long periods of time (>1 Ma on average), tectonic strain is ~10% on average and does not vary significantly along axis. There is a marked asymmetry across the axis in tectonic strain, with ~50% lower tectonic strain on the east flank than on the west flank, which is likely due to highly asymmetric magmatic accretion on axis as deduced from deeptow magnetic data [51].

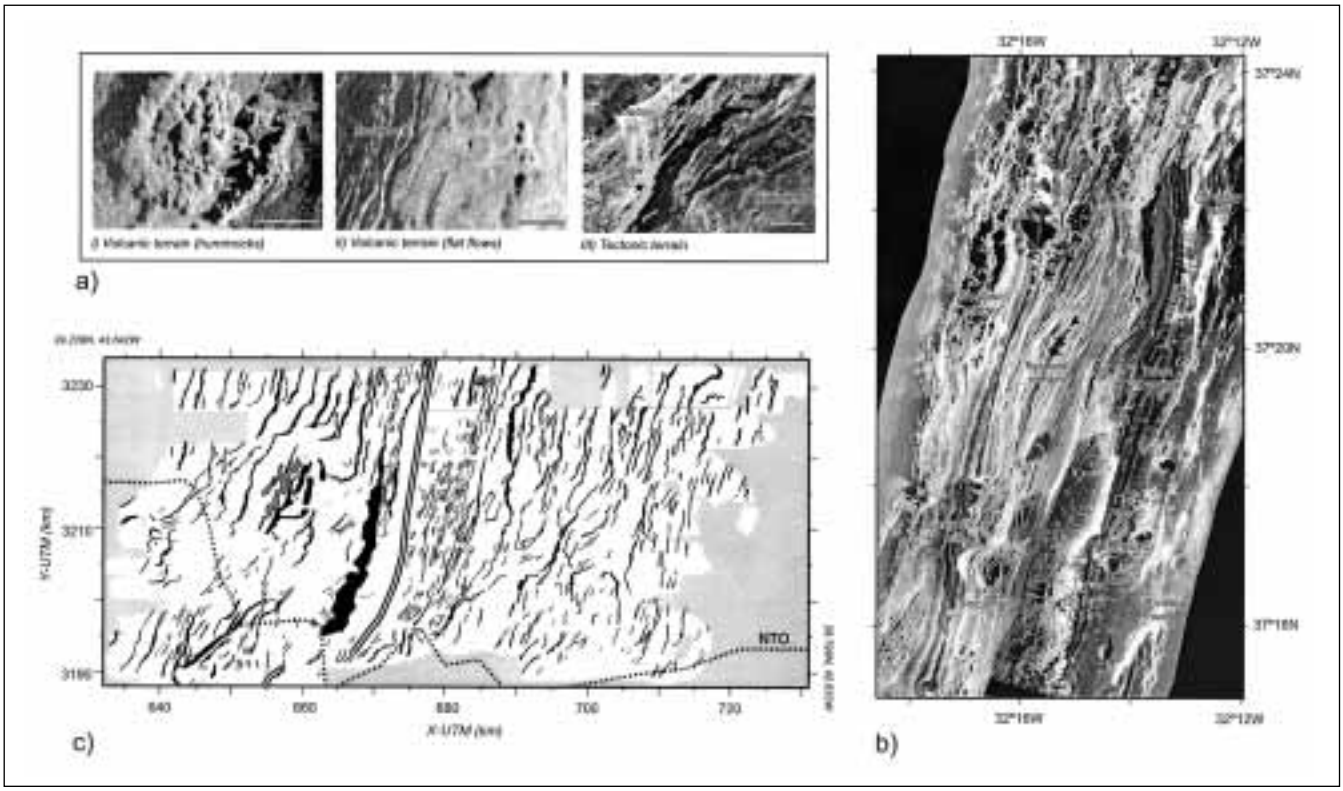

Figure 4. a) Seafloor textures as identified on high-resolution sidescan sonar images from the deep-towed TOBI system: (I) hummocky volcanic terrain, (II) flat lava flows with fissures and small-scale faulting and (III) tectonic terrain with large fault scarps and mass-wasting deposits associated. Bars correspond to 0.5 km. b) Interpreted TOBI sidescan sonar image along the axial valley of the Lucky Strike segment, MAR South of Azores. The insonified area is about 6 km wide. Reflective surfaces, such as high-relief areas or rock outcrops are white, whereas less reflective surfaces, such as sedimented areas, are dark-grey. Acoustic shadows are black. The central volcanic platform corresponds to the locus of magmatic accretion. Axial-parallel fissures and faults indicate near-axis tectonic extension within the valley floor. Modified from [40]. c) Fault map of the Broken Spur ridge segment, Mid-Atlantic Ridge (29°N) interpreted from a TOBI sidescan sonar mosaic. Double line is the ridge axis, and the dotted line marks the NTO trace bounding the segment to the South. Black: inward-facing faults; grey: outward-facing faults. Modified from [50].

These variations in tectonic strain do not correlate directly with changes in fault spacing and heave. Fault spacing and heave increase from the center of the segment towards the IC on the west flank, and from the OC to the IC across the axis (Fig. 4c). These parameters remain relatively constant along the segment on the east flank, and across the axis at the segment center. Tectonic strain appears to be decoupled from magmatic strain at a >1 Ma time scale, as the decrease in magma supply from the segment center towards the end (inferred from variations in crustal thickness along the axis) is not correlated with a complementary increase in tectonic strain. On the contrary, tectonic strain remains relatively constant along the axis at ~7% on the east flank, and at ~15% on the west flank. These results indicate that variations in fault development may reflect spatial differences in the rheology of the lithosphere, and not changes in tectonic strain or magma supply along-axis [50].

MAR at Fifteen-Twenty Fracture Zone, 15°20'N

The MAR is deepest near the Equator, suggesting a relatively cold mantle unaffected by hotspots. The Fifteen-Twenty Fracture Zone (FTFZ) and adjacent ridge segments correspond to the possible location of the triple junction between the North-American (NAM), South American (SAM) and African (AFR) plates (Figs. 1, 3a,d), which migrated northward from the Marathon FZ (10°N) to the 14°N-16°N area [52,53]. South of the FTFZ, the axial valley is formed by a series of *en échelon* deeps 8-18 km long, and of short axial volcanic ridges (e.g. 14°40'N, 45°02'W). North of the fracture zone, the axial valley is more linear, with a long axial volcanic ridge north of 15°45'N. Axial depths increase gradually towards the FTFZ (Fig. 5a), with no marked relative bathymetric highs and lows defining ridge segmentation as in other areas of the MAR [9] (Fig. 5).

Both north and south of the FTFZ, there is a transition from a 'linear' terrain with long abyssal hills that are sub-parallel to the ridge axis, to a 'rugged' terrain with short and oblique fault scarps [54]. The 'rugged' terrain is found at either side of the FTFZ, with south-propagating V-shaped transitions to the 'linear' terrain distant from the FTFZ (at ~15°50'N and ~14°30'N). At greater off-axis distances, the terrain is 'rugged' and the transition disappears. The change in tectonic pattern is correlated with variations in rock types (Fig. 5a). Extensive outcrops of serpentinized peridotite and gabbro, found at <~60 km from the FTFZ and on both flanks, correspond to a thin magmatic crust (Fig. 5b,c) and a crust compositionally and mechanically heterogeneous [55]. These outcrops are capped by a thin (<500 m) layer of extrusive basalt [54]. This suggests along-axis variation in lithospheric composition and tectonic pattern in the area,

with substantially more peridotite at shallow levels of the crust in the 'rugged' terrain near the FTFZ, and a more magmatic crust away from it, in the 'linear' terrain, which is consistent with the crustal thickness patterns deduced from gravity data. (Fig. 5a,b).

The detailed bathymetric maps also reveal the presence of corrugated surfaces (Fig. 5a), from 10 to 15 km across-axis and up to 25 km along axis, with striations sub-parallel to the spreading direction at wavelengths of <3 km, and later high-angle faults cutting it. Similar structures were first described near the Atlantis Fracture Zone [12,56,57] and found later in other MORs [e.g., 56-59]. They are regarded as the exposed surfaces of long-lived detachment faults that tectonically uplift ultramafic rocks [12,56], which is consistent with gabbro and peridotite exposures over the detachment at 15°45'N [60] uplifted from deep structural levels. While oceanic detachments elsewhere mostly occur at ICs [12,56,57], in the 15°N region they occur on both flanks of the axis and away from the FZ, and are not associated with any NTO.

Geological and geophysical observations in the FTFZ area suggest that the magma supply to the crust is reduced. Amagmatic plate separation results in a very thin magmatic crust, a lithosphere with large amounts of peridotites tectonically accreted, and the formation of low-angle, long-lived normal faults.

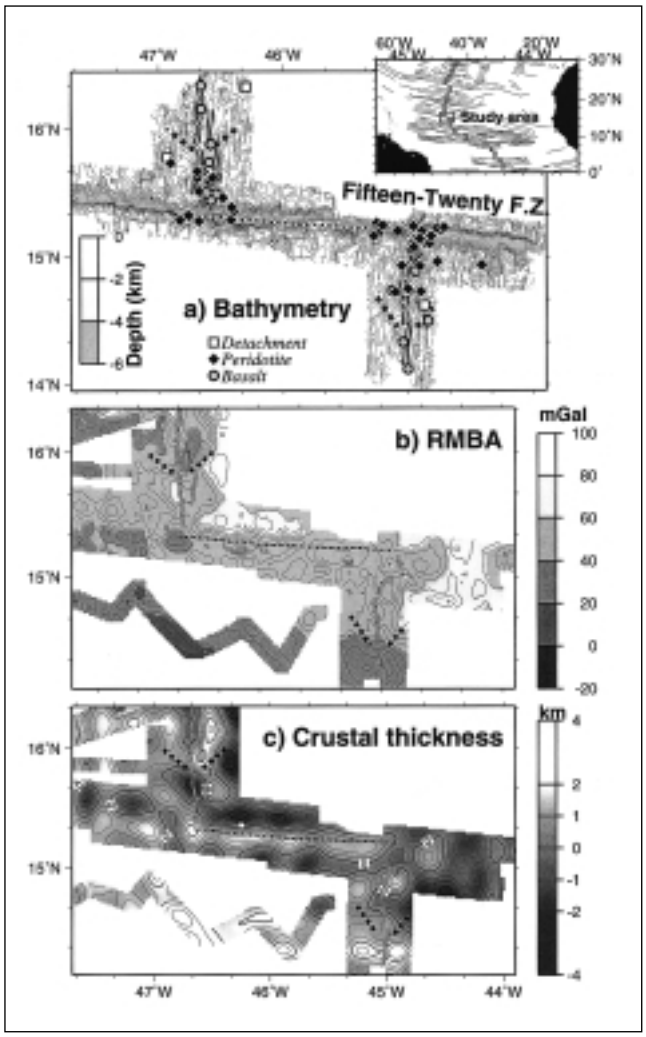

Figure 5. a) Bathymetry, b) residual mantle Bouguer gravity anomaly and c) inferred crustal thickness around the Fifteen-Twenty Fracture Zone, Mid-Atlantic Ridge. a) Bathymetric map and dredge locations. Extensive exposures of peridotites on the seafloor indicate a thin and discontinuous magmatic crust and a restricted melt supply to the ridge axis. The area is also characterized by the presence of low-angle detachment faults. b) The residual gravity anomaly map shows «bull's eye» gravity lows (thick crust) away from the fracture zone, and an irregular pattern close to it. c) The crust is thicker over the gravity lows (see b) and immediately below the transform valley. The lows are likely due to focused magmatic accretion (thicker magmatic crust), while fracturation and serpentinization may account for the alteration of the shallow mantle, resulting in an apparently thick crust at this location. Melt supply is generally reduced close to the fracture zone. Modified from [55].

The Bransfield and North Fiji Backarc Basins

Two backarcs are presented in this section. They are extreme examples in the evolution of backarc basins. The Bransfield Basin (BB) is an extensional basin developing within a continental volcanic arc in the Antarctica, whereas the North Fiji Basin (NFB) is one of the maturest active marginal basins in the Southwest Pacific (Fig. 1, Table 1).

The Central Bransfield Basin

The BB is a narrow and elongated basin behind the South Shetland Trench, separating the South Shetland Islands from the Antarctic Peninsula (Fig. 6a). This area, located at the south-western tip of the Scotia Arc (Fig. 6a), is one of the most accessible parts of the Antarctica. Since the first geophysical investigations carried out in the 1970's [61], the geodynamics of this area has been extensively studied.

The BB is more than 400 km long, limited by the extension of the Hero and Shackleton Fracture Zones, and up to 80 km wide, between the longitudes 62°W and 54°W and the latitudes 61°S and 64°S (Fig. 6a). It has been suggested that the BB is opening because, when the Antarctic-Phoenix ridge stopped spreading 4 Ma ago, the subducting plate (former-Phoenix Plate, Fig. 6a) continued to sink by oceanward migration of the hinge of subduction [62-65]. Trench rollback results in the opening of the basin, and so its extent would be similar to the amount of extension in the basin. Some authors [e.g. 63] suggested that extension started between 4 and 1.3 Ma ago. Although magnetic anomalies are difficult to identify in the BB, a central positive anomaly along the basin axis has been observed. Crustal ages ranging from 1.3 to 1.8 Ma and spreading rates from 2.5 to 9 mm/yr have been suggested [66-68]. Morphologically, the BB consists of three small basins, Western, Central and Eastern, separated by the Deception and Bridgeman islands [69] (Fig. 6b). Here we focus on the largest, the Central Bransfield Basin (CBB), which has been studied using swath-bathymetric systems by the «*Geociències Marines*» group of the University of Barcelona [70-71].

The CBB is about 40 km wide, 230 km long, and 1950 m deep. It is characterized by progressive deepening towards the northeast with a smooth, step-like topography [71] (Fig.

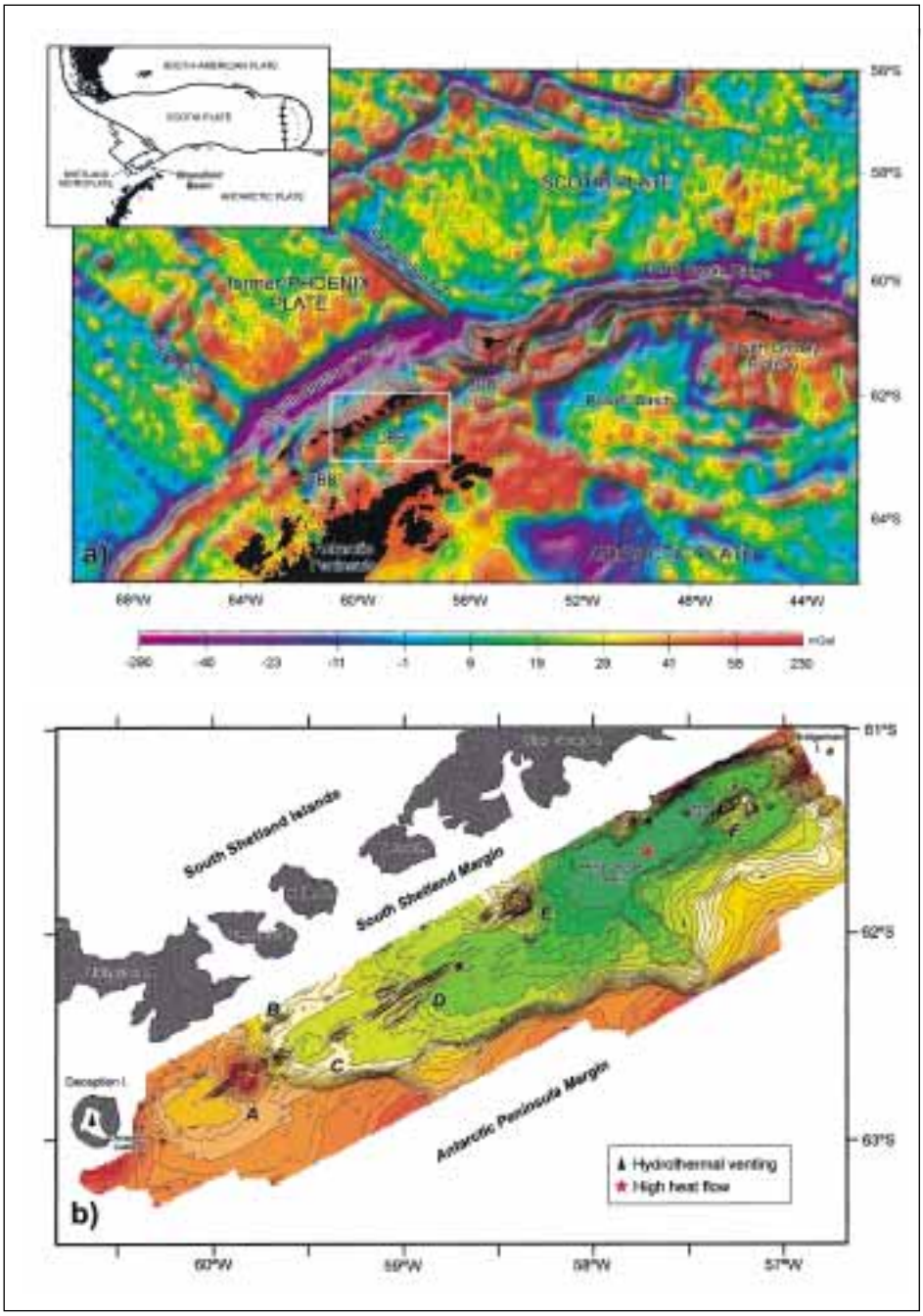

Figure 6. a) Location map of the Bransfield Basin at the NW Antarctic Peninsula region, based on satellite gravity data (10 mGal contour) [31]. Inset: Present-day plate tectonic setting of the Bransfield Basin. WBB: Western Bransfield Basin; CBB: Central Bransfield Basin; EBB: Eastern Bransfield Basin. b) Swath-bathymetric map of the Central Bransfield Basin (50 m contour), modified from [70,71]. A to F denote the large volcanic edifices (up to 0.5 km high) and ridges identified along the axis of the basin. Hydrothermal activity is found at the flanks of edifice F and within the Deception Caldera [73]. The highest heat flow values are found at the center of the King George Basin [65].

6b). The margins of the CBB are highly asymmetric: the South Shetland Islands margin is narrow, steep (up to 24°), rectilinear (trending N65°) and corresponds to the northwest boundary of the basin rift. In contrast, the Antarctic Peninsula margin is wide (70-85 km), sinuous, and gently deepens into the basin (Fig. 6b). On the basin floor, six large seamounts (labeled A to F) rise above the sedimented seafloor [71] (Fig. 6b). The seamounts are volcanic edifices, as supported by their morphology, the nature of their dredged samples [72] and seismic facies [e.g., 69]. Most of the edifices have been sampled and fresh, glassy basalts no older than 300,000 years have been systematically recovered [72]. Evidence of hydrothermal activity has recently been detected in the water column and in the sediments near edifice F [73], where high heat flow measurements (up to 626 mW/m^2) have been recorded [65].

The volcanic edifices are parallel to the basin axis (N55-N60) and are located at the intersection with transverse-trending structures. The volcanoes show different morphologies, from circular (<15 km of diameter, <550 m high) to elongated (<15 km long, 3.5 km wide, <350 m high) [74]. Edifice E shows a clear conical and caldera-shaped morphology with spurs trending N55-N60. Edifice A is formed by a split caldera the two halves of which keep their original shapes. Between both halves, there is a ridge formed by coalescence of point source volcanoes, as suggested by detailed bathymetric data [71]. Edifice D, consisting of three parallel ridges, may correspond to a further stage of extension and propagation of volcanism where the initial volcano would have lost its original shape. The edifices on the CBB clearly illustrate how volcanism and tectonics interplay at the axis of an extensional basin [74].

The North Fiji Basin

The NFB is the large, triangular basin located at the boundary between the Pacific and the Indo-Australian plates, between two active subduction zones of opposite polarity: the New Hebrides and the Tonga-Kermadec trenches (Fig. 7a). Located between longitudes 168°E and 180°E, and latitudes 10°S and 25°S, the basin extends along 1200 km from north to south, and 700 km from west to east. Large-scale heat flow and seismicity studies carried out there during the 60's and 70's, supported the hypothesis of basin formation by seafloor spreading [e.g., 75]. Several models have been proposed to explain the geodynamic evolution of the NFB [76-78], but all of them suggested that the basin opened at least 10 Ma ago as a result from the clockwise rotation of the New Hebrides Arc and the anti-clockwise rotation of the Fiji Islands, after the dismemberment of a unique arc. Thereafter, different trending spreading systems started within the basin. Recent studies in the frame of international scientific programs [79-80] have recognized several extensional structures and active spreading centers in the NFB. Two of them, the Central Spreading Ridge (CSR) and the South Pandora Ridge (SPR) are presented here (Fig. 7).

The Central Spreading Ridge

The CSR is the best developed, in terms of structure and magmatism, of all the spreading centers identified in the basin, and may be one of the largest spreading systems of the west Pacific backarc basins (Fig. 7a). It has been intensively explored during the French-Japanese STARMER project (1987-1992) [80]. Magnetic anomalies indicate that seafloor spreading began at the central part of the ridge about 3.5 Ma ago. About 1.5 Ma ago, changes in the geodynamic setting and a successive plate-motion reorganization resulted in the present ridge segmentation [81-82]. Basalts accreted along the CSR are predominantly MORB-type, although there is a geochemical backarc signature on the northern and southern part of the spreading center [83]. There is extensive low-temperature hydrothermal activity, in addition to some sites of vigorously active high temperature venting along the CSR [84].

The CSR, 800 km long and up to 60 km wide, is segmented into three first order segments named from North to South according to their orientation, N160, N15 and NS [81,82,85] (Fig. 7b). They are bounded by four main discontinuities: the 14°50'S and 16°50'S triple junctions [85,86], and the 18°10'S

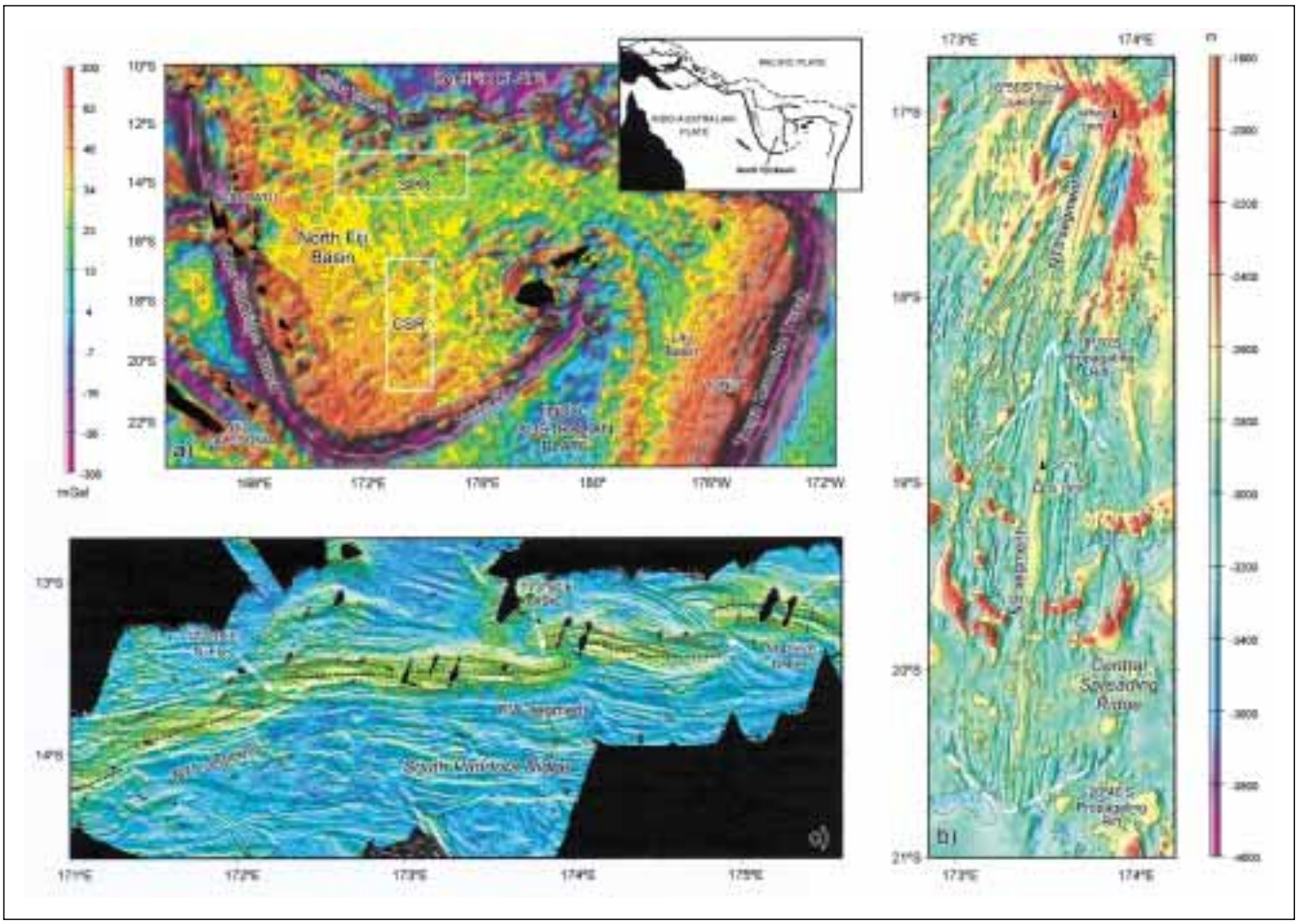

Figure 7. a) Location of the Central Spreading Ridge and South Pandora Ridge (CSR and SPR, respectively) on the North Fiji Basin, based on satellite gravity data (10 mGal contour) [31]. Inset: Present-day plate tectonic setting of the Southwest Pacific. b) Swath-bathymetric shaded relief map of the Central Spreading Ridge, showing two first order segments and axial discontinuities (triple junctions and ridge propagators). Triangles depict hydrothermal sites (black, high temperature venting site; white, fossil hydrothermal site). Modified from [75]. c) Acoustic backscattering map of the South Pandora Ridge, which has an average spreading rate of 8 mm/yr. Modified from [93]. Green corresponds to high reflectivity areas (i.e. young lavas, high relief), whereas blue corresponds to less reflective areas (i.e. sediments, flat areas).

and 20°40'S propagating rifts [87]. The axial morphology changes from a succession of long and deep *en échelon* grabens (N160 segment) similar to the MAR; to a dome split by an axial graben (N15 segment); to a central flat top high (NS segment), like the EPR (Fig. 7b). Magnetic anomalies up to Anomaly 2A (3.5 Ma) are recognized along the NS segment, whereas only Anomalies J and 1 (0.97 and 0.7 Ma, respectively) are identified along the other two segments. The calculated spreading rate is intermediate, decreasing northwards from 83 mm/yr at 20°30'S to 50 mm/yr at 17°S [82]. There is also a change in the gravity structure between the northern and southern segments of the CSR. The MBA obtained in the northern part of the CSR (N160/N15 segments) show «bull's eyes» structures, regarded as focused accretion at the segment centers, and crustal thickness variations between the center and the segment ends [9]. In contrast, the MBAs resulting at the NS segment are more homogeneous, probably associated with a more constant along-axis crustal thickness. The strong contrast in bathymetry and gravity structure between the segments, with an intermediate spreading rate, reflects differences in the magma supply and ridge thermal regime [88].

The South Pandora Ridge

The SPR is located at the northern part of the NFB, one of the less explored areas of the basin (Fig. 7a). The ridge was first identified on the basis of only magnetic anomaly identification [89], although more recently, bathymetric and gravity profiles [90], petrology of dredged samples [91] and sidescan sonar facies [92], have revealed that SPR is an active spreading center. The axis of the SPR and flanks up to 7 Ma old were accurately surveyed by the NOFI cruise of *RV L'Atalante* [93], during which swath-bathymetry, geophysical and geological data were acquired.

The SPR extends over more than 450 km and consists of two first-order segments, named according to their orientation (N75 and E-W), separated by NTOs and OSCs (Fig. 7c). The axial domain, characterized by high reflectivity on the acoustic backscatter map (Fig. 7c), is dominated by the alternation of large seamounts and deep troughs. The ridge flanks are characterized by numerous volcanic constructions, up to several kilometers in diameter, and a cyclic succession of E-W trending lineations parallel to the spreading axis, interpreted as fault scarps (Fig. 7c). Magnetic anomalies 1 to 3A (7 Ma) have been identified along the SPR, with an ultra-slow spreading rate of 16 mm/yr [93]. The gravity structure also shows «bull's eye» gravity lows associated with the axial highs at the center of the segments.

Discussion and Conclusions

Some authors believed that seafloor spreading at backarcs was more diffuse than at MORs [76,94-96], although both are zones of oceanic accretion characterized by relatively shallow seafloor, elevated heat flow, shallow microseismic activity, similar segmentation patterns, and recognizable axis-parallel magnetic lineations [97-99]. In both cases, the magmatic crust is about 6 km thick, and consists of a layer of basalt flows and dykes (MORBs, upper crust), underlain by intrusive gabbros (lower crust) [77,98,99].

All these similarities indicate that the same accretion processes operate in both systems. Thus, the study of both backarc and MORs provides complementary data on factors controlling the mode of crustal accretion. In this section we will discuss, first, the segmented nature of the magma supply to the ridge axis; second, crustal construction and its interaction with segmentation; and third, the hydrothermal

Table 2. Morphotectonic and geological characteristics of the six study areas.

Ridge name	*Spreading rate* (mm/yr)	*Depth (average)* (m)	*Morphologic features*	*Discontinuities*	*Hydrothermal vent sites*	*References*
Mid-Atlantic Ridge						
1. South Azores (38°N-35°40'N)	24 (slow)	2700	rift valley, axial seamount	fracture zone, NTO	Menez Gwenn, Lucky Strike, Rainbow	34, 38, 39, 119
2. South Atlantis FZ (29°N)	26 (slow)	3200	rift valley axial volcanic ridge	fracture zone, NTO	Broken Spur	45, 50, 118
3. Fifteen-Twenty (15°20'N)	26 (slow)	3800	rift valley detachment	fracture zone, NTO	Logachev	54, 55, 120
North Fiji Basin						
4. South Pandora R.	16 (ultra-slow)	3100	rift valley, axial high	OSC, NTO	?	93
5. Central Spr. Ridge	50-80 (intermediate)	2700	rift valley, axial dome	propagator, NTO, triple junction	White Lady, St.14	77, 78, 84, 85, 87, 88
Bransfield Basin						
6. Central Basin	< 10? (ultra-slow)	1500	axial seamounts, volcanic ridges	volcanic gap	Hook Ridge (Low T) Deception caldera	65, 71, 73, 74

activity involved in the cooling and alteration of the oceanic lithosphere.

Ridge Discontinuities: Segmented Magma Supply to the Crust

The initial rifting of the continental crust seems to pre-determine the overall geometry of the ridge axis, as suggested for the Northern MAR [100], or some backarcs, e.g. Sumisu Rift [101] and the northern Mariana Trough [102]. Once seafloor spreading is operating, volcanic activity is highly focused forming a narrow zone (< 20 km) of crustal accretion and is organized along discrete segments. The average spacing between volcanic edifices in the incipient CBB is 25 to 30 km (Figs. 6b, 8a). This is of the same order as the average segment length (ranging from 10 to 100 km) found for the slow spreading MAR [e.g., 3]. Thus, since early seafloor spreading, magma supply is segmented with a characteristic spacing of tens of km [25]. Thicker crust is found at the center of the slow spreading segments [9,11], indicating melt focusing in the upper astenosphere/lower lithosphere [27,103]. Accretion in fast spreading ridges is also segmented, but the characteristic ridge segment length is longer (at least 100 km), and crustal thickness is relatively constant along the axis. The presence of a shallow and continuous axial melt lens indicates a higher magma supply than at slow ridges, and provides also a mechanism to distribute melt along the axis.

Backarc systems are smaller (<1000 km) and younger (< 10 Ma) than MORs (>1000 km and <180 Ma). However, ridge segments are bound by the same type of discontinuities, including OSCs, propagating rifts, NTOs and devals [3,4,6,25,87,104-107] (Fig. 7b,c). Because of the short lifespan and rifting history of backarcs, no large fracture zones are recognizable. The ultra-slow SPR (Fig. 7c) is characterized by OSCs that are very similar to those found at the fast EPR [105]. These structures are reorganizations of the neovolcanic ridge at discontinuities, and require significant magma budget. Therefore, magma budget is independent of spreading rate and requires enhanced melting of the mantle. The presence of water from the subducting slab in the mantle can lower the temperature of melting [108], thus

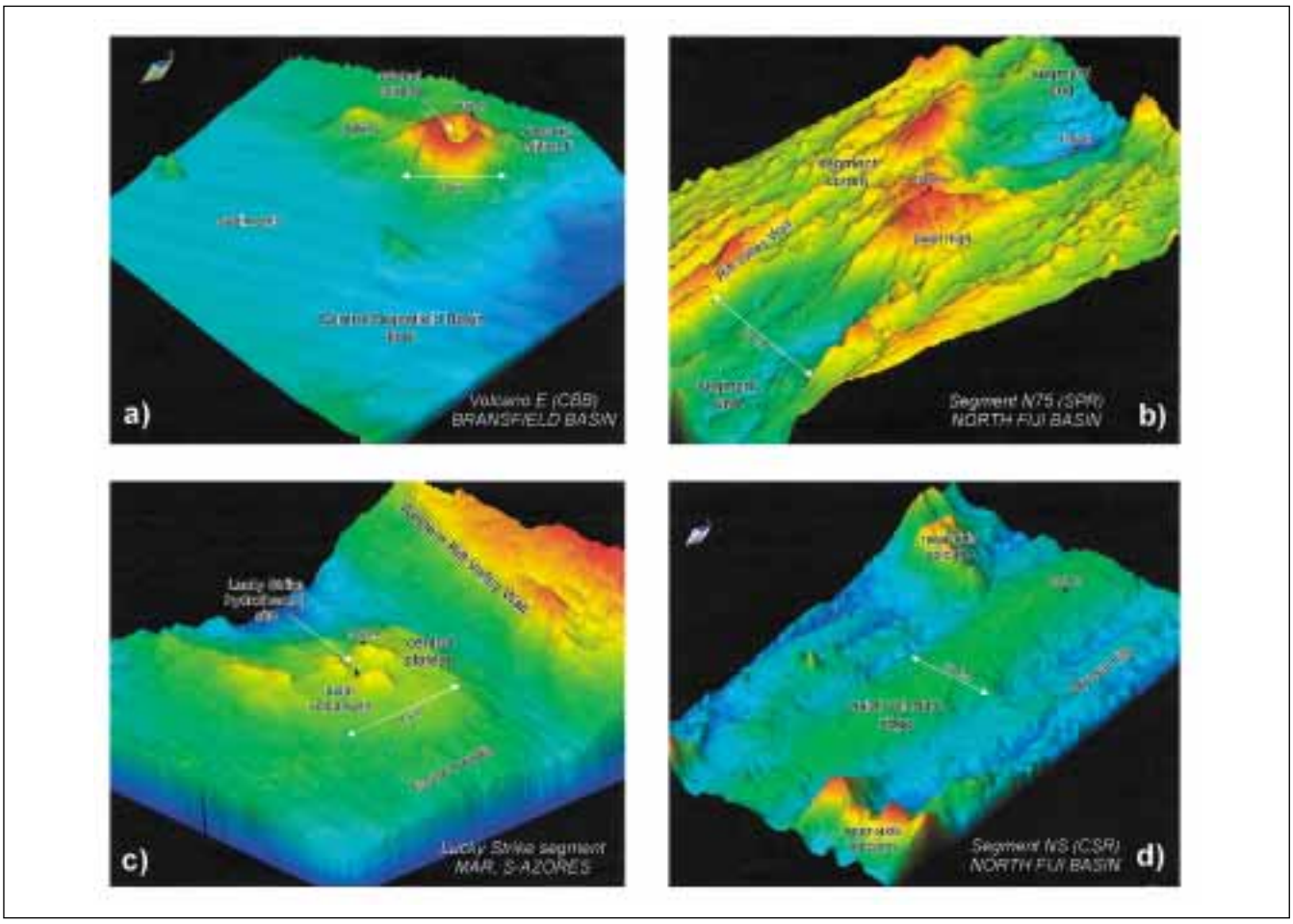

Figure 8. Colour-shaded 3D-views of portions of the areas studied, showing differences in the relative importance of magmatic and tectonic processes. a) Volcanic edifice E at the foot of the South Shetland Margin, Central Bransfield Basin. Modified from [70]; b) Detail of the N75 trending segment of the South Pandora Ridge (North Fiji Basin) showing a central volcanic high occupying the rift valley floor. Linear abyssal hills result from extensive axis-parallel faulting of the crust, destroying axial volcanic edifices. Based on data from [93]; c) Central volcanic platform within the rift valley floor of the Lucky Strike segment (Mid-Atlantic Ridge, south of to the Azores). High temperature hydrothermal venting has been found within the three axial constructions. Modified from [38]; d) Typical morphology of a fast-spreading ridge at the NS segment, Central Spreading Ridge (North Fiji Basin). Note the lack of extensive faulting, and the presence of near-axis volcanoes. Based on data from [78,88]. These figures were made at DRO/GM, IFREMER-Brest, France.

producing larger amounts of melt at backarcs than at MORs for a given spreading rate.

Processes of Crustal Accretion

The structure and composition of the oceanic lithosphere is the result of the interplay of the magmatic and tectonic processes which take place near the ridge axis, which are controlled by spreading rate, magma supply and other factors mentioned above, and are organized at the scale of individual segments. Seafloor morphology, acoustic backscatter and geological observations provide constrains on these accretionary processes.

Volcanic Construction of the Crust at the Ridge Axis

The upper magmatic crust is constructed by eruption of magma to the seafloor. For example, along slow-spreading ridges unaffected by hotspots, there is a predominance of seamount construction, which coexists locally with fissure eruptions and small flows [44,109]. In contrast, in fast-spreading ridges, fissure eruptions producing sheet-flows seem to dominate the construction of the upper crust [5,18,105] although seamounts on –and off–axis also exist. In addition to spreading rate, the volcanic construction of the upper crust also depends on the magma supply and thickness of the brittle lithosphere, among other factors.

At the slow-spreading MAR, individual seamounts, typically about 100 m high and < 2 km of diameter, coalesce to form continuous axial volcanic ridges (AVR), about 200 m high and < 5 km wide [e.g., 109,110] (Fig. 4c). Axial seamounts are interpreted as single volcanic eruptions from a small magma chamber. This indicates that magmatism is discontinuous in time but concentrated along a narrow zone about the ridge axis (e.g., South Atlantis FZ and Fifteen-Twenty portions of the MAR), with no evidence of off-axis volcanism [110].

In contrast, seamounts at the MAR South of Azores, CBB and SPR are significantly higher (> 150 m) and larger (>10 km) than at other zones of MAR, isolated without coalescing and forming AVRs (Figs. 4b, 8a,b,c). In these cases, seamounts result from larger magma chambers, and/or several volcanic eruptions due to more effective melt focusing than in the South Atlantis FZ or Fifteen-Twenty areas. In the MAR South of Azores, the ridge axis shoals to less than 1500 m of depth, and the axial rift valley disappears due to the hotspot influence. Therefore, enhanced melt supply to the ridge axis is consistent with larger magma chambers and larger volcanic edifices. In the case of the CBB and SPR, eruptions initiate and focus into single volcanic vents, controlled by structural trends within the basin (Figs. 6b, 7c, 8a,b). Construction of the upper extrusive crust at the intermediate spreading CSR is similar to that found at fast spreading ridges [111] (Fig. 8d), where most of the crust is constructed by sheet-flows and fed from fissure eruptions above a steady-state magma chamber lying continuous along-axis. Chains of large off-axis seamounts are also found locally associated with the most magmatic sections of segments (Figs. 7b, 8d).

In addition to spreading rate or magma supply, the thickness of the brittle lithosphere is also involved in the mode of volcanic construction. Near the Azores, where the magma supply is high and the spreading rate is slow, the thick brittle lithosphere prevents the formation of a continuous, steady-state axial melt lens [40]. Instead, seamounts are fed from plutonic intrusions within the lower crust. In the presence of a shallow melt lens, there is a very thin (< 2 km) brittle layer that prevents melt from focussing to form individual seamounts. Instead, fissure eruptions uniformly distribute melt along the axis.

The construction of the magmatic lower crust cannot be directly constrained from the data presented here. However, from geological and geophysical observations, the lower crust, both at fast –and slow–ridges, is the result of cooling of magmatic intrusions or and/or crystal fractionation. With decreasing magma supply, plate separation cannot be taken up totally by magmatic accretion, resulting in thinner magmatic crust and accretion of mantle lithosphere [109].

Tectonic Emplacement of the Lithosphere

Plate separation is partially taken up by tectonic extension, as demonstrated by the high resolution images of the interaction between volcanism and faulting at the ridge-axis (Fig. 4a, b). Faulting is initiated within the axial valley in the form of small scale fissures and short faults with small throw. Deformation is established by linkage and growth of smaller faults within the rift valley walls and beyond to form the ridge-parallel abyssal hill pattern (Fig. 4c). For example, the tectonic strain calculated at 29°N is about 10% of the total plate separation, with variations in fault geometry associated with the rheological structure of the lithosphere (see section 3.2) [50].

In the extreme case of very low magma supply (e.g. Fifteen-Twenty), magmatic crust is thin (< 4 km), and peridotites crop out at the seafloor close to the ridge axis. The presence of mantle rocks at shallow levels of the lithosphere requires a very effective tectonic mechanism to produce several km of vertical uplift within less than 10 km from the ridge axis [54,112]. This may be achieved by a set of short-lived cross-cutting normal faults under the axial valley [54]. Another proposed mechanism is the effective localization of deformation along long-lived, low-angle detachment faults [113]. This detachments, about 10 to 30 km wide and with extension-parallel striations [12], expose upper mantle and lower crustal rocks uplifted from deep structural levels at time scales between 1 and 3 Ma [56,114]. These structures are also common along the Fifteen-Twenty area [55] (Fig. 5). Mantle outcrops are also found near ridge discontinuities of «normal» slow spreading segments, where magma supply is also low because of focused accretion [56,57,115].

Cooling and Alteration of the Lithosphere: Hydrothermal Activity

Active hydrothermal systems are common at MORs and backarcs (Table 2). They are driven by magmatic heat sources under the axis, and are a fundamental process to

remove heat from the oceanic lithosphere resulting in the alteration of rocks [116]. There are different types of hydrothermal systems, depending on the thermal regime (high T (350°C) or low T (< 350°C)) and the geological setting (hosted in volcanic or ultramafic rocks). These are end-member models, and the combination of two or more of them has been suggested [117].

The hydrothermal sites of Menez Gwenn and Lucky Strike (South of Azores) (Fig. 8c), Broken Spur (South Atlantis FZ) and White Lady (CSR) are high temperature and hosted in basaltic rocks [38,39,73,84,85,118]. Hook Ridge at the CBB is also hosted in basalts (Fig. 6b), but flow is diffuse and the water is low temperature [73]. The Rainbow (South of Azores) [119] and Logachev (Fifteen-Twenty) sites [120] are both high temperature systems hosted in ultramafics rocks. In this case, water chemistry from the plume shows that, in addition to the interaction between water and a heat source, there is active hydration of the peridotite during serpentinization, and thus, CH_4 degassing [121,122]. Nevertheless, there is not a clear correlation between magma supply and abundance, spatial distribution, and type of hydrothermal sites. The local tectonic control of permeability enhances fluid circulation and favors serpentinization and high-temperature hydrothermal venting [116,119].

Acknowledgements

We would like to thank the Principal Investigators, chief scientists, captains, officers, and crew who made possible the cruises which are the source of the data presented in this paper, especially Jean-Marie Auzende, Miquel Canals, Mathilde Cannat, Yves Lagabrielle, Lindsay Parson, and Roger Searle. We thank Mathilde Cannat and Jian Lin for constructive comments and reviews, and Salvador Reguant for his suggestions throughout the different stages of this article. The authors acknowledge the funds from the Commissionat per a Universitats i Recerca – Generalitat de Catalunya to EG, the Ministerio de Educación y Cultura to JE, and the Dept. of Geophysics (ICTJA-CSIC) through ref. 1997SGR00020 to JE and EG.

References

[1] Müller, R.D., Roest, W.R., Royer, J.-Y., Gahagan, L.M., Sclater, J.G., 1997. Digital isochrons of the world's ocean floor. *J. Geophys. Res., 102*, 3211-3214.

[2] Heezen, B. C., Tharp, M., 1965. Tectonic fabric of the Atlantic and Indian Oceans and continental drift. *Phil. Trans. R. Soc. London, 258*, 90-106.

[3] Schouten, H., Klitgord, K.D., Whitehead, J.A., 1985. Segmentation of mid-ocean ridges. *Nature, 317*, 225-229.

[4] Macdonald, K.C., Fox, P.J., 1983. Overlapping spreading centres: New accretion geometry on the East Pacific Rise. *Nature, 302*, 55-58.

[5] Macdonald, K.C., 1986. The crest of the Mid-Atlantic Ridge: Models for crustal generation and tectonics. *In:* Vogt, P.R., Tucholke, B.E., (Eds.), *The Geology of North-America, The Western North Atlantic Region*. Geol. Soc. Amer., vol. M, 51-68.

[6] Hey, R., 1977. A new class of «pseudofaults» and their bearing on plate tectonics: a propagating rift model. *Earth Planet. Sci. Lett., 37,* 321-325.

[7] Schouten, H., Klitgord, K.D., Gallo, D.G., 1993. Edge-driven microplate kinematics. *J. Geophys. Res.*, 98, 6689-6701.

[8] Macdonald, K.C., 1982. Mid-ocean ridges: Fine-scale tectonic, volcanic and hydrothermal processes within the plate boundary zone. *Annual Review of Earth and Planetary Sciences*, *10*, 155-190.

[9] Lin, J., G. M. Purdy, H. Schouten, J. C. Sempere, C. Zervas, 1990. Evidence from gravity data for focused magmatic accretion along the Mid-Atlantic Ridge. *Nature, 344,* 627-632.

[10] Detrick, R.S., White, R.S., Purdy, G.M., 1993. Crustal structure of North-Atlantic fracture zones. *Rev. Geophys., 31,* 439-459.

[11] Tolstoy, M., Harding, A. J., Orcutt, J.A., 1993. Crustal thickness on the Mid-Atlantic ridge: Bull's eye gravity anomalies and focused accretion. *Science, 262*, 726-729.

[12] Cann, J. R., Blackman, D.K., Smith, D.K., McAllister, E., Janssen, B., Mello, S., Avgerinos, E., Pascoe, A.R., Escartín, J., 1997. Corrugated slip surfaces formed at North Atlantic ridge-transform intersections. *Nature, 385,* 329-332.

[13] Dick, H.JB., Thompson, W.B., Bryan, W.B., 1981. Low angle faulting and steady-state emplacement of plutonic rocks at ridge-transform intersections. *EOS, Trans. AGU, 62*, 406.

[14] Cannat, M., Casey, J.F., 1995. An ultramafic lift at the Mid-Atlantic Ridge: Successive stages of magmatism in serpentinized peridotites from the 15°N region. *In:* Vissers, R.L.M. and Nicolas, A. (Eds.), *Mantle and lower crust exposed in oceanic ridges and in ophiolites*. Kluwer Academic publishers, Netherlands, 5-34.

[15] Cannat, M., 1993. Emplacement of mantle rocks in the seafloor at mid-ocean ridges. *J. Geophys. Res., 98*, 4163-4172.

[16] Cannat, M., Mével, C., Maia, M., Deplus, C., Durand, C., Gente, P., Agrinier, P., Belarouchi, A., Dubuisson, G., Humler, E., Reynolds, J., 1995. Thin crust, ultramafic exposures, and rugged faulting patterns at the Mid-Atlantic Ridge (22°-24°N). *Geology, 23,* 49-52.

[17] Chen, Y., 1992. Oceanic crustal thickness versus spreadig rate. *Geophys. Res. Lett.,* 19, 753-756.

[18] Hooft, E.E.E., Detrick, R.S., Kent, G., 1997. Seismic structure and indicators of magma budget along the southern East Pacific Rise. *J. Geophys. Res., 102,* 27319-27340.

[19] Detrick, R.S., Kent, G.M., Orcutt, J.A., Mutter, J.C., Buhl, P., 1993b. Seismic structure of the southern East Pacific Rise. *Science, 259*, 499-503.